The Principle and Practical Progress of 3D Printing Technology in Knee Joint and Meniscus

Zelin Liu [1, *] and Xiaohan Yang [2]

[1] Guangdong Pharmaceutical University, Guangzhou, China

[2] Hangzhou Wickham International School, Hangzhou, China

* Corresponding Author Email: 2230503133@stu.gdpu.edu.cn

Abstract. Repairing meniscus tears poses significant challenges, impacting normal knee joint movement and potentially leading to secondary osteoarthritis over time. The limited availability of donor tissue, coupled with issues such as graft rejection, results in an inadequate supply for meniscus tissue replacement and regeneration in patients. This context has led to the development of regenerative scaffolds. Advances in 3D printing technology for cartilage tissue regeneration have enabled the creation of intricate meniscus scaffolds with high precision and biological activity. These scaffolds effectively mimic the extracellular matrix (ECM) and cartilage, ultimately facilitating meniscus regeneration by providing structural support and promoting cell attachment, proliferation, and differentiation. This paper primarily discusses the applications of 3D printed meniscus tissue engineering scaffolds in regenerative medicine, introducing and comparing various examples of 3D printing technologies and raw materials. Additionally, we examine the performance requirements for meniscus scaffolds, address existing challenges and limitations, and consider prospects in this field.

Keywords: 3D printing, knee joint, meniscus.

1. Introduction

The meniscus is a crescent-shaped, wedge-like structure composed of fibrocartilaginous tissue, situated between the femoral condyle and the tibial plateau, covering approximately two-thirds of the tibial plateau. The peripheral regions of the meniscus are vascularized, comprising about 10-25% of its total volume in adults. These areas receive blood supply from adjacent joint capsules and synovial vessels, while the remaining regions have limited vascularization and primarily depend on nutrients from synovial fluid [1, 2]. Composed of 72-77% water, the meniscus has a dry weight that is 85-95% collagen, predominantly type I and type II [1, 3]. Its surface is covered with a thin layer of cartilage, while the internal structure consists of fibrocartilaginous components, including collagen fibers and chondrocytes. The outer collagen fibers are primarily organized in a circular pattern, whereas a smaller number of inner fibers are arranged radially. These structural characteristics endow the meniscus with considerable tensile strength, allowing it to convert vertical longitudinal stress into transverse circumferential stress, thereby withstanding axial loads on the joint [4]. During knee flexion and extension, the meniscus adapts to changes in shape as it contacts the femoral articular surface, minimizing incongruence in the knee joint, increasing the contact area, and distributing pressure across joint surfaces. Notably, the anterior portion of the meniscus exhibits a greater damping capacity than the relatively fixed posterior portion, underscoring the meniscus's critical role in knee joint mechanics [5].

Meniscus injury involves the rupture of this crescent-shaped fibrous cartilage. Degeneration due to prolonged wear or acute trauma can lead to partial or complete loss of function, disrupting normal knee movement and potentially resulting in secondary osteoarthritis over time. Historically, total meniscectomy has been the primary treatment following a definitive diagnosis. While immediate outcomes may be satisfactory, long-term consequences due to altered load transmission can lead to the development of osteoarthritis (OA). In the United States, over one million patients undergo surgical repair or meniscectomy annually, with approximately 50% of those with meniscal injuries progressing to OA within 10 to 20 years post-injury [6]. Compared to the vascularized regions that can heal, nearly two-thirds of the meniscus comprises the white zone (avascular region), which has

limited healing capacity and may extend into the red-white zone, further complicating meniscal injuries. While allograft transplantation may be an option following meniscectomy, significant challenges such as donor scarcity, pathogen transmission, and immune rejection remain [1].

The advancement of 3D printing technology for cartilage tissue regeneration represents a significant innovation in medical science, utilizing 3D printing techniques to fabricate customized cartilage tissues. Central to this technology is the creation of biologically active cartilage structures and scaffolds. High-resolution 3D printing enables the production of tiny porous spheres made from biocompatible, biodegradable materials, which can be embedded with stem cells. Over time, these cells proliferate within the spheres, filling the entire volume and forming densely packed living cellular constructs. These constructs can be arranged into predetermined shapes, allowing the cells to merge and grow together, ultimately resulting in uniform, seamless, and homogenous cartilage tissue. This method addresses the limitations of previous technologies by providing precise control over the shape and structure of artificial cartilage. It offers a novel approach to overcoming donor site deficiencies in meniscus transplantation, paving the way for personalized cartilage repair and regenerative medicine in the future [7].

2. 3D Printing Technology Related to Knee Repair

3D printing has a wide range of applications in knee joint repair, and different printing technologies and printing materials have a decisive impact on the performance of meniscus scaffold (Table 1).

Table 1. Three Scheme comparing

Technologies	Material	Merits	Ref.
3DPI (inkjet 3D printing)	Collagen and PCL	Providing support and strength for the developed tissue; beneficial for cell viability.	[8]
	Dextran ink, TPU ink, carbon black, Ag:Pa ink, soft PDMS ink, rigid PDMA ink	Controllable viscosity and corresponding wetting and spreading behavior; mimicking the structure of the native heart.	[9]
	Pepsin solubilized liver dECM bioink, PCL	Induce hepatic differentiation and enhance hepatocyte-specific functions.	[10]
	Alginate/Gelatin	Good biocompatibility, biodegradability, easy functionalization and fast gelling behavior; rheological properties can be easily adjusted by different concentrations and the use of additives and other polymers.	[11]
	Sacrificial carbohydrate glass with fibrin gel cast	Give rise to a functionally significant collateral circulation; increased vascularization.	[12]
FDM	PCL-MECM 1andKGN-loaded PLGA	Superior meniscus regeneration; Excellent cell affinity, preserving cell vitality and chondrogenic activity.	[13]
	PCL 1 CTGF and TGF-β3	Induce spatial fibrochondrocyte differentiation; Produce physiological anisotropy in the engineered meniscus; Long-term chondroprotection of knee joint.	[14]
SLA (stereo lithography appearance)	PDLLA-PEG and HA	Enables the precise arrangement of cells and bioactive molecules in space and simulates complex physiological structures.	[15]
	GelMA, GM-HA:GelMA	Hexagonal hepatic lobule units printed with GelMA and patterned supportive cells in sinusoidal regions printed with GM-HA/GelMA.	[16]
LDM (low-temperature deposition manufacturing)	Bio-ceramic materials	Withstand greater pressure and load; good compatibility with human tissue; adjustable degradation rate.	[17]
	Water-based polyurethane (WPU), ECM	Creating biochemical and biomechanical targets; hierarchical macro-micro porous structure.	[18]
Micro-Extrusion	Calcium alginate (Alg-Ca), and dextran methacrylate derivatives (dex-MA)	Higer Young moduli; excellent hydrophilic; good flow properties; enhance specific tissue formation by embedded cells.	[19]
	blend of alginate and GelMA	Maintain shape fidelity; increase elastic modulus.	[20]

2.1. Inkjet Printing

Currently, the most widely used 3D printing systems are based on droplet-based inkjet printing technology. This approach leverages physical properties such as piezoelectricity, acoustics, and electrostatics to disintegrate printing materials into streams of droplets, which are then deposited layer by layer to create three-dimensional structures [21]. In the realm of 3D bioprinting, the relatively low cost and straightforward design of inkjet printing have made it a favored method in many laboratories for manufacturing cellular structures with spatial pattern control. By alternating between bioprinter ink and crosslinking agent solutions during the printing process, and subsequently employing physical or chemical means for crosslinking, highly bioactive 3D scaffolds can be fabricated. Compared to other printing technologies, inkjet printing excels at constructing complex cellular tissues and scaffolds from a variety of bioprinting materials, including biomaterials, cells, growth factors, drugs, and genes. Moreover, inkjet printers are versatile, cost-effective, and user-friendly, demonstrating significant translational potential for clinical applications. However, this technology necessitates low-viscosity hydrogel materials to prevent nozzle clogging, which can result from uneven droplet sizes and adhesion. Additionally, mechanical and thermal stresses may compromise the bioactivity of the materials, impeding the formation of structures with high biological density, while high concentrations of bioink can complicate the achievement of optimal mechanical strength and structural integrity [21].

2.2. Extrusion-based printing

2.2.1. Fused Deposition Modelling (FDM)

FDM is one of the most widely employed additive manufacturing techniques and is particularly efficient for fabricating physical three-dimensional thermoplastics [22]. Its advantages include rapid production speeds, cost-effectiveness, accessibility, and a broad adaptability to various materials. In the FDM process, thermoplastic materials are heated to a molten state and extruded layer by layer onto a platform from a nozzle with a diameter ranging from approximately 0.1 mm to 1 mm, following a CAD model [22, 23]. After extrusion, the material cools and solidifies, bonding with previously deposited layers to create a stable structure. Nonetheless, FDM encounters challenges such as reduced vertical strength due to temperature fluctuations and warping, which can lead to inter-layer separation. Additionally, the relatively thick extruded layers result in a rough surface finish, often necessitating extra support for structural stability [24]. Furthermore, the machine's operational temperature, typically around 300°C, limits the ability to print materials with higher melting points.

2.2.2. Liquid Deposition Modelling (LDM)

LDM is a green manufacturing process that does not involve heating for liquefaction and can produce scaffolds with controllable pore structures at multiple scales and interconnected micropores, making it widely applicable in bone tissue engineering. The extruder used in LDM typically operates at room temperature and can be either piston-based or pneumatic. Scaffolds are manufactured layer by layer on a cold platform or within a freezer, with the solvent subsequently removed through freeze-drying. Compared to conventional extrusion methods, LDM facilitates permanent cross-linking of the solution with the polymer during cold gelation, leading to the formation of microporous structures upon thawing, which enhances cell and tissue adhesion and growth [25]. Key advantages of LDM include the ability to control pore size by selecting appropriate solvents or precursor solutions, as well as low-temperature deposition, which preserves the activity of growth factors and cells. However, the mechanical properties of scaffolds produced via LDM are generally weaker than those fabricated through FDM. Additionally, the low-temperature deposition, typically below 0°C, limits the range of suitable solvents, complicating the attainment of a homogeneous solution containing both natural and synthetic polymers [26].

2.2.3. Micro-extrusion Printing

Micro-extrusion printing utilizes a pump, piston, and screw to apply pressure to a syringe filled with bio-ink, allowing for layer-by-layer continuous extrusion and solidification of the bio-ink through a nozzle. By controlling parameters such as pressure, nozzle size, and printing speed, one can achieve good spatial resolution and high bioactivity in complex tissue structures [27, 28]. The nozzle can achieve an accuracy of up to 1 μm, enabling sub-millimeter resolution and moderate-speed movement, with the capability to switch between multiple nozzles made from different materials. While spiral micro-extrusion printing accommodates a wider range of high-viscosity and shear-thinning bio-inks compared to traditional extrusion methods, it still faces challenges. High shear stress from excessive extrusion pressure can diminish cellular viability and structural integrity [29]. Additionally, when compared to laser-assisted printing, extrusion printing generally exhibits lower resolution, and achieving high accuracy can be costly.

2.3. Laser-assisted Printing (LAB)

LAB offers the ability to fabricate in vitro tissue models characterized by high resolution, rapid printing speeds, substantial cell density, and elevated cell viability [28]. A primary technique in laser-assisted technology is laser-induced forward transfer (LIFT), which utilizes two parallel glass slides: a donor (upper) slide and a collector (lower) slide. The donor slide contains the biological material, while the collector slide is coated with a metallic material (such as gold, titanium, or silver) that absorbs laser energy. Upon laser pulse absorption, the biological material is propelled onto the collector slide, forming a 3D model, with laser energy typically ranging from 65 nJ to 190 μJ [30]. The Gaussian distribution of laser intensity enables resolution below the diffraction limit, facilitating the formation of high-quality nanostructures with dimensions smaller than 100 nm. The bioprinting inks associated with LIFT typically consist of combinations of alginate, glycerol, and ethylenediaminetetraacetic acid, and studies have shown that LAB technology can successfully construct tissue structures utilizing biological materials with viscosities ranging from 1 to 400 mPa·s [31].

2.4. Optical Projection Stereolithography (OPSL)

OPSL employs dynamic OPSL (DOPsL) or continuous liquid interface production (CLIP) as layerless printing methods [32, 33]. DOPsL technology involves projecting maskless patterns onto the surface of biomaterials, enabling the simultaneous printing of all structures for each layer in a single exposure. Digital micromirror devices (DMD), consisting of millions of independently controlled mirrors, generate high-precision maskless patterns [32]. While DOPsL technology is efficient and performs excellently, it requires realignment and recalibration after each layer is completed. In contrast, CLIP technology enables uninterrupted object printing by creating a continuous liquid interface (a dead zone) with an oxygen-permeable window beneath the UV image projection plane. The oxygen-rich dead zone suppresses radical photopolymerization between the window and the polymerizing portions, allowing for continuous exposure as the print rises [34]. This projection-based approach enhances the smoothness of formed structures compared to nozzle-based printing, significantly improving printing speed and spatial resolution [28]. Currently, OPSL technology is applied in tissue engineering to print complex cellular biostructures encapsulating patterns formed by cells. However, it has yet to successfully manufacture complex natural tissue structures with cellular and biomaterial diversity. Bio restorative resins used in visible-light polymerization (VP) bioprinting typically consist of solvent water, photoreactive monomers or oligomers, and photo initiators (PIs), with viscosities ranging from 10−1 to 10 Pa·s [35]. While low-viscosity bio restorative resins facilitate the printing process, they may also lead to undesired cell sedimentation over prolonged bioprinting, resulting in uneven cellular distribution within the printed structures [36]. Consequently, selecting appropriate PIs and biomaterials for bio restorative resin formulation is critical for enhancing printing accuracy and reducing manufacturing times.

3. Performance Required for the Meniscus Scaffold

3D-printed meniscal tissue scaffolds can be categorized into synthetic, natural, and composite types. These scaffolds must possess specific biological properties to facilitate the repair of meniscal cartilage injuries. Understanding the mechanisms underlying meniscal cartilage repair—such as mechanical properties, scaffold design, bioactivity, and biocompatibility—is crucial for developing advanced scaffolds. This section will elaborate on these distinct mechanisms.

3.1. Mechanical Properties

Recent research has increasingly focused on biomechanical stimulation to create a simulated physiological microenvironment for meniscal scaffolds. Evaluating the mechanical performance of these scaffolds allows for assessment of their strength, stiffness, and performance under dynamic loading conditions, providing insights into how biomechanical stimulation influences cellular behavior and tissue formation. This understanding is vital for advancing mechanically simulated scaffolds.

The meniscus functions to convert compressive loads from the femur into circumferential tensile stresses, necessitating scaffolds with corresponding capabilities. Meniscal cartilage scaffolds are therefore required to exhibit robust mechanical properties, with a compressive modulus of 75-150 kPa and a tensile modulus of 75-150 MPa [5]. These scaffolds often incorporate hydrogels, porous polymeric materials, extracellular matrix (ECM) components, and synthetic materials to enhance mechanical performance, typically utilizing one or more materials to achieve superior mechanical properties. For instance, Li et al. demonstrated that a combination of polycaprolactone (PCL) and silk fibroin (SF) exhibited enhanced mechanical properties compared to pure SF scaffolds, which significantly underperformed relative to natural menisci. Moreover, scaffolds modified with PS-L7 showed a greater elastic modulus compared to pure PS scaffolds [37].

The incorporation of biomolecules into meniscal scaffolds can enhance chondrocyte activity, leading to improved regenerative outcomes and biomechanical performance. Additionally, inorganic factors can induce biomolecule generation, optimizing scaffold mechanical properties. For example, incorporating strontium (Sr) into PCL-SF scaffolds notably upregulated collagen type II gene expression in stem cells[fig.1A], significantly enhancing the scaffolds' biomechanical performance (Fig. 1) [38]. Other studies have utilized bioprinting with materials exhibiting varied mechanical properties to replicate the anisotropic characteristics of natural meniscal tissue [5], ensuring prolonged supportive functionality post-implantation [39].

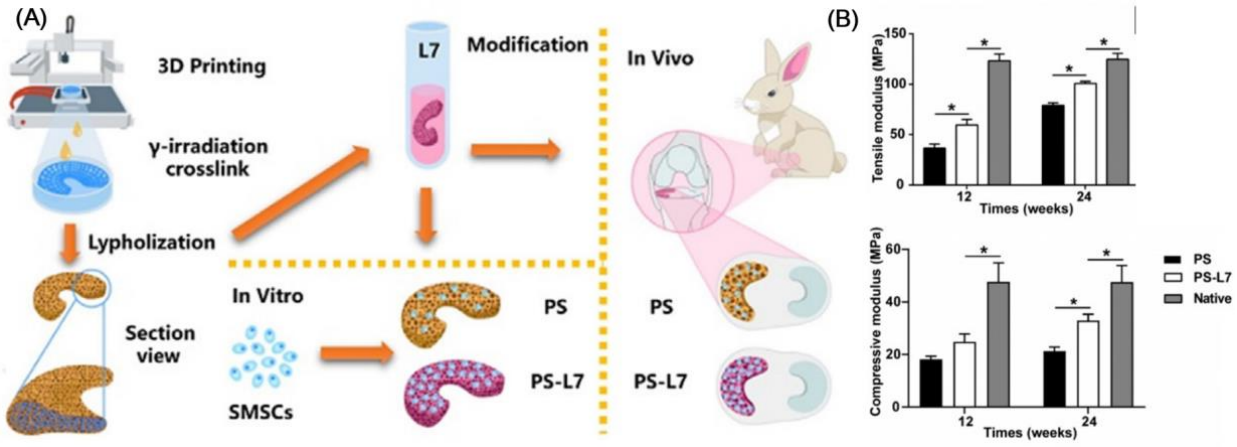


Figure 1. PS-L7 scaffold preparation and biomechanical measurements [38].

Bioinspired scaffolds can also provide cells with biomechanical cues, altering cell morphology and enhancing activity. Chen et al. employed a water-based LDM method to construct a water-based polyurethane (WPU)-ECM hybrid scaffold with a hierarchical macro-micro porous structure. This scaffold's porous architecture creates biochemical and biomechanical targets that promote the proliferation of endothelial stem progenitor cells (ESPCs) and their differentiation into chondrocytes,

leading to a gradual improvement in the Young's modulus of the repaired tissue, thereby closely resembling the mechanical properties of native menisci after six months [18].

Furthermore, bioprinted scaffolds can facilitate the stepwise release of growth factors, mimicking biochemical signaling to stimulate collagen production. Lee et al. demonstrated a stepwise release of connective tissue growth factor (CTGF and TGFβ3) within scaffolds, which promoted the recruitment of endogenous mesenchymal stem cells (MSCs) to knee wounds and enhanced collagen I mRNA expression via FAK signaling (Fig. 2). This resulted in a multifunctional distribution of collagen and glycosaminoglycans (GAGs) within the meniscus, effectively simulating the native distribution of cartilage-supporting components (Figure 2) [14].

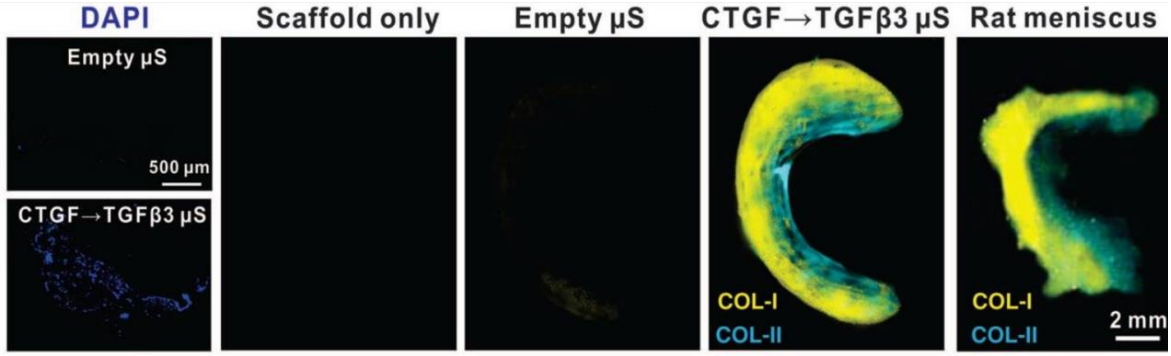


Figure 2. When the scaffold was incubated on a single layer of human MSC for 6 weeks, the step-by-step delivery of CTGF and TGF-β3 induced cells to form region-specific collagen type I and II substrates, which like natural rat meniscus [14].

3.2. Biodegradability

In addition to favorable mechanical properties, the degradability of cartilage scaffolds is a critical focus of research. Scaffold degradation creates space for newly formed tissue to regenerate; ideally, the degradation period for a cartilage scaffold should range from 9 to 12 months [40]. The integration of 3D printing technology with biodegradable polymers has enabled the design of complex scaffolds for regenerating various tissues and organs, including bone, cartilage, cardiac, and nervous tissues.

For meniscus scaffolds, 3D-printed hybrid material scaffolds can achieve optimal graded degradation, effectively promoting structural regeneration. Guo et al. developed acellular PCL-MECM scaffolds, where the majority of the MECM degraded completely within one-month post-implantation, while residual PCL scaffolds remained visible after three months [41]. This degradation timeline provides sufficient time for cell differentiation necessary for in vivo chondrogenesis before the MECM is fully degraded. Meanwhile, the residual PCL scaffolds continue to offer biomechanical support, addressing complex mechanical demands over an extended in vivo period (Fig. 3).

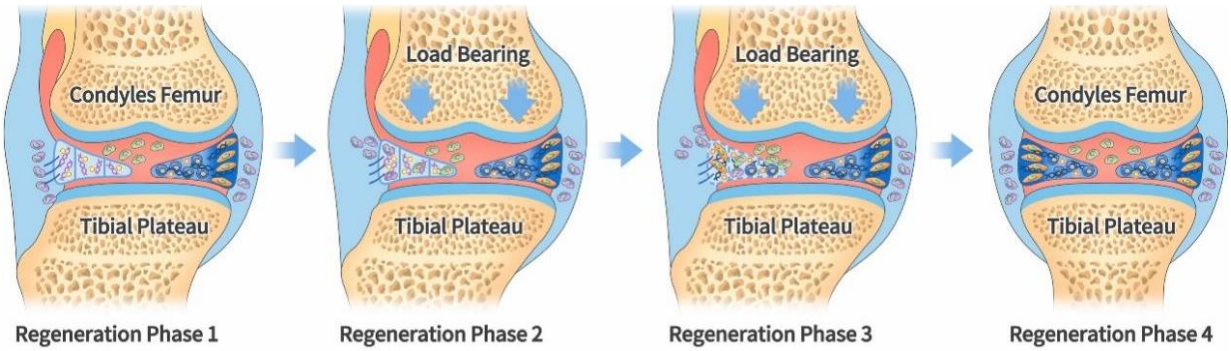


Figure 3. PCL-MECM scaffold degradation process [41]

Research indicated that the early inflammatory response triggered by scaffold implantation recruits macrophages, which, through the regulation of macrophage polarization, can accelerate scaffold degradation and enhance tissue regeneration. Chen utilized decellularized meniscus matrix as bioink to construct a novel tissue-engineered meniscus scaffold featuring a hierarchical microstructure with

large and micropores via LDM [42]. After one week of implantation, a mild inflammatory response was observed, gradually diminishing over three weeks, accompanied by partial degradation of the scaffold.

Furthermore, studies have shown that highly absorbent scaffolds can expedite the hydrolysis of specific scaffold materials. One study revealed that the weight loss of synthetic polymer scaffolds was significantly lower than that of gelatin scaffolds with high water absorption, indicating that moisture facilitates the hydrolysis of gelatin and cross-linked polymers within the scaffolds [43]. Additionally, structural changes during scaffold degradation can lead to cracks, increasing the eroded surface area and accelerating the hydrolysis process.

While microporous structures are known to enhance cellular activity and mechanical properties [18], their impact on scaffold degradation may be minimal. Literature suggests that there are no significant differences in the degradation rates of three-dimensional meniscus scaffold models with pore sizes of 215 μm, 320 μm, and 515 μm [44].

3.3. Biocompatibility

Scaffolds composed of biomaterials such as gelatin, chitosan, collagen, chondroitin, hyaluronic acid, and extracellular matrix (ECM) components demonstrate good biocompatibility and are less likely to provoke immune responses. For meniscus regeneration or its substitutes, scaffold materials must exhibit both biocompatibility and bioactivity. Numerous evaluations of biocompatibility have been conducted on various PCL-based and non-PCL-based scaffolds for meniscus replacement. Gopinathan et al. assessed the biocompatibility of carbon nanofiber crosslinked PCL scaffolds with meniscus cells, noting that individual cells maintained a spherical morphology within scaffold pores [45]. However, when the scaffold was functionalized with biomolecules, alterations in cell morphology were observed. In vivo studies using a rabbit model demonstrated that despite firm adhesion of the scaffold to the tissue, vascularization occurred in the surrounding tissue layers, indicating that biomolecule-functionalized PCL scaffolds enhance meniscus cell viability.

Research also suggests that sustained-release technology can effectively mimic the in vivo microenvironment over time, thereby improving scaffold biocompatibility. One study prepared composite scaffolds from PCL, ECM components, and PLGA microspheres loaded with kartogenin (KGN) to promote endogenous cell differentiation [13]. The biomimetic microenvironment created by the continuous release of KGN significantly enhanced the chondrogenesis of synovial mesenchymal stem cells (SMSCs), facilitated ECM formation, optimized scaffold microstructure, and improved cell adhesion and proliferation in a hydrophilic environment.

Recent studies have reported that PCL/hydrogel scaffolds exhibit excellent biocompatibility, with a relatively high DNA content indicating cell quantity observed two weeks post-implantation [40]. The hydrogel provided a protective effect on cells; after eight weeks of incubation with porcine tissue, significant ECM deposition was noted within the scaffold among chondrocytes. Guo et al. cultured meniscus fibro chondrocytes on PCL-ECM scaffolds, with SEM results demonstrating good cell adhesion, high ECM secretion, and favorable biocompatibility [41]. While smaller pore sizes enhanced cell adhesion, excessively small pores (e.g., 215 μm) led to substantial internal cell deaths due to inadequate nutrient supply during the initial stages, with 320 μm performing better [44].

Additionally, a scaffold utilizing a nanofiber array mimicking the circumferential and radial arrangements of the inner and outer meniscus regions induced cell growth along the fiber distribution [46]. This approach provides topological guidance and biophysical cues essential for the regeneration and development of meniscal tissue.

4. Conclusion

Despite significant advancements in 3D-printed meniscus scaffolds, challenges remain, including uncontrollable growth factor release, mismatches in mechanical properties, and insufficient printing accuracy. The specific tissue structures of the human body are composed of distinct cells and tissues,

making the selection of appropriate cells crucial for successful 3D bioprinting. However, not all tissue-specific cells can be isolated and cultured in vitro, nor can all cells maintain their biological activity in the 3D printing environment. Optimizing cell separation, culture, and proliferation techniques is therefore essential for enhancing the success of 3D bioprinting.

Furthermore, various tissues and organs exhibit unique physical and mechanical properties, necessitating the selection of biomaterials that correspond to these characteristics. These materials must also sustain the biological activity and function of the chosen cells, presenting an additional challenge for 3D bioprinting technology in biomaterial selection.

While several 3D printing technologies are widely used in medicine, many still face technical limitations. For instance, the resolution and speed of 3DPI can restrict fidelity and clinical applicability, whereas extrusion-based 3D printing, while offering high speeds, requires improvements in cell density and biocompatibility.

3D bioprinting technology integrates the knowledge of manufacturing science with biomedicine, representing a high-tech field at the intersection of both disciplines. This technology has successfully transitioned from basic research to practical application, with successful transplantation of 3D-printed ears, blood vessels, bones, and muscle tissues into experimental animals, and its implementation across various levels of medical practice. Looking ahead, 3D bioprinting is poised to evolve towards higher precision and personalized customization.

Authors Contribution

All the authors contributed equally and their names were listed in alphabetical order.

References

[1] Baker B, Gee A, Sheth N, et.al. Meniscus Tissue Engineering on the Nanoscale –From Basic Principles to Clinical Application. Journal of Knee Surgery, 2009, 22 (01): 45 – 59.

[2] Makris E A, Hadidi P, Athanasiou K A. The knee meniscus: Structure–function, pathophysiology, current repair techniques, and prospects for regeneration. Biomaterials, 2011, 32 (30): 7411 – 7431.

[3] Cheung H S. Distribution of Type I, II, III and V in the Pepsin Solubilized Collagens in Bovine Menisci. Connective Tissue Research, 1987, 16 (4): 343 – 356.

[4] Petersen W, Tillmann B. Collagenous fibril texture of the human knee joint menisci. Anatomy and Embryology, 1998, 197 (4): 317 – 324.

[5] Pereira H, Caridade S G, Frias A M, et.al. Biomechanical and cellular segmental characterization of human meniscus: building the basis for Tissue Engineering therapies. Osteoarthritis and Cartilage, 2014, 22 (9): 1271 – 1281.

[6] Tarafder S, Park G, Lee C H. Explant models for meniscus metabolism, injury, repair, and healing. Connective Tissue Research, 2019: 1 – 12.

[7] Ozbolat I T, Peng W, Ozbolat V. Application areas of 3D bioprinting. Drug Discovery Today, 2016, 21 (8): 1257 – 1271.

[8] Lee J W, Choi Y-J, Yong W-J, et.al. Development of a 3D cell printed construct considering angiogenesis for liver tissue engineering. Bio fabrication, 2016, 8 (1): 015007.

[9] Lind J U, Busbee T A, Valentine A D, et.al. Instrumented cardiac micro physiological devices via multimaterial three-dimensional printing. Nature Materials, 2016, 16 (3): 303 – 308.

[10] Lee H, Han W, Kim H, et.al. Development of Liver Decellularized Extracellular Matrix Bioink for Three-Dimensional Cell Printing-Based Liver Tissue Engineering. Biomacromolecules, 2017, 18 (4): 1229 – 1237.

[11] Duan B, Hockaday L A, Kang K H, et.al. 3D Bioprinting of heterogeneous aortic valve conduits with alginate/gelatin hydrogels. Journal of Biomedical Materials Research Part A, 2012, 101A (5): 1255 – 1264.

[12] Mirabella T, MacArthur J W, Cheng D, et.al. 3D-printed vascular networks direct therapeutic angiogenesis in ischemia. Nature Biomedical Engineering, 2017, 1 (6).

[13] Li H, Liao Z, Yang Z, et.al. 3D Printed Poly(ε-Caprolactone)/Meniscus Extracellular Matrix Composite Scaffold Functionalized with Kartogenin-Releasing PLGA Microspheres for Meniscus Tissue Engineering. Frontiers in Bioengineering and Biotechnology, 2021, 9.

[14] Lee C H, Rodeo S A, Fortier L A, et.al. Protein-releasing polymeric scaffolds induce fibrochondrocytic differentiation of endogenous cells for knee meniscus regeneration in sheep. Science Translational Medicine, 2014, 6(266).

[15] Suri S, Han L-H, Zhang W, et.al. Solid freeform fabrication of designer scaffolds of hyaluronic acid for nerve tissue engineering. Biomedical Microdevices, 2011, 13 (6): 983 – 993.

[16] Ma X, Qu X, Zhu W, et.al. Deterministically patterned biomimetic human iPSC-derived hepatic model via rapid 3D bioprinting. Proceedings of the National Academy of Sciences, 2016, 113 (8): 2206 – 2211.

[17] Baino F, Fiume E. 3D Printing of Hierarchical Scaffolds Based on Mesoporous Bioactive Glasses (MBGs)—Fundamentals and Applications. Materials, 2020, 13(7): 1688.

[18] Chen M, Li Y, Liu S, et.al. Hierarchical macro-microporous WPU-ECM scaffolds combined with Microfracture Promote in Situ Articular Cartilage Regeneration in Rabbits. Bioactive Materials, Elsevier BV, 2021, 6 (7): 1932 – 1944.

[19] Pescosolido L, Vermonden T, Malda J, et.al. In situ forming IPN hydrogels of calcium alginate and dextran-HEMA for biomedical applications. Acta Biomaterialia, Elsevier BV, 2011, 7 (4): 1627 – 1633.

[20] Colosi C, Shin S R, Manoharan V, et.al. Microfluidic Bioprinting of Heterogeneous 3D Tissue Constructs Using Low-Viscosity Bioink. Advanced Materials, 2015, 28 (4): 677 – 684.

[21] Gudapati H, Dey M, Ozbolat I. A comprehensive review on droplet-based bioprinting: Past, present and future. Biomaterials, 2016, 102: 20 – 42.

[22] Bol R J M, Šavija B. Micromechanical Models for FDM 3D-Printed Polymers: A Review. Polymers, 2023, 15 (23): 4497.

[23] Wang, Zhao, Fuh, et.al. Effect of Porosity on Mechanical Properties of 3D Printed Polymers: Experiments and Micromechanical Modeling Based on X-Ray Computed Tomography Analysis. Polymers, 2019, 11 (7): 1154.

[24] Rajan K, Samykano M, Kadirgama K, et.al. Fused deposition modeling: process, materials, parameters, properties, and applications. The International Journal of Advanced Manufacturing Technology, 2022, 120.

[25] Wubneh A, Tsekoura E K, Ayranci C, et.al. Current state of fabrication technologies and materials for bone tissue engineering. Acta Biomaterialia, 2018, 80: 1 – 30.

[26] Liu W, Wang D, Huang J, et.al. Low-temperature deposition manufacturing: A novel and promising rapid prototyping technology for the fabrication of tissue-engineered scaffold. Materials Science and Engineering: C, Elsevier BV, 2017, 70: 976 – 982.

[27] Lee S, Son M, Lee J, et.al. Computational Fluid Dynamics Analysis and Empirical Evaluation of Carboxymethylcellulose/Alginate 3D Bioprinting Inks for Screw-Based Micro extrusion. Polymers, MDPI AG, 2024, 16 (8): 1137.

[28] Yu C, Zhu W, Sun B, et.al. Modulating physical, chemical, and biological properties in 3D printing for tissue engineering applications. Applied Physics Reviews, 2018, 5(4): 041107.

[29] Blaeser A, Duarte Campos D F, Puster U, et.al. Controlling Shear Stress in 3D Bioprinting is a Key Factor to Balance Printing Resolution and Stem Cell Integrity. Advanced Healthcare Materials, 2015, 5 (3): 326 – 333.

[30] Alonzo M, AnilKumar S, Roman B, et.al. 3D Bioprinting of cardiac tissue and cardiac stem cell therapy. Translational Research, 2019, 211: 64 – 83.

[31] Gruene M, Unger C, Koch L, et.al. Dispensing pico to nanolitre of a natural hydrogel by laser-assisted bioprinting. BioMedical Engineering OnLine, 2011, 10 (1): 19.

[32] Zhang A P, Qu X, Soman P, et.al. Rapid Fabrication of Complex 3D Extracellular Microenvironments by Dynamic Optical Projection Stereolithography. Advanced Materials, 2012, 24 (31): 4266 – 4270.

[33] Huang J, Qin Q, Wang J. A Review of Stereolithography: Processes and Systems. Processes, 2020, 8 (9): 1138.

[34] Janusziewicz R, Tumbleston J R, Quintanilla A L, et.al. Layerless fabrication with continuous liquid interface production. Proceedings of the National Academy of Sciences, 2016, 113 (42): 11703 – 11708.

[35] Li Y, Zhang X, Zhang X, et.al. Recent Progress of the Vat Photopolymerization Technique in Tissue Engineering: A Brief Review of Mechanisms, Methods, Materials, and Applications. Polymers, Multidisciplinary Digital Publishing Institute, 2023, 15 (19): 3940 – 3940.

[36] Mondschein R J, Kanitkar A, Williams C B, et.al. Polymer structure-property requirements for stereolithographic 3D printing of soft tissue engineering scaffolds. Biomaterials, 2017, 140: 170 – 188.

[37] Li Z, Wu N, Cheng J, et.al. Biomechanically, structurally and functionally meticulously tailored polycaprolactone/silk fibroin scaffold for meniscus regeneration. Theragnostic, 2020, 10 (11): 5090 – 5106.

[38] Li Y, Chen M, Zhou W, et.al. Cell-free 3D wet-electrospun PCL/silk fibroin/Sr2+ scaffold promotes successful total meniscus regeneration in a rabbit model. Acta Biomaterialia, Elsevier BV, 2020, 113: 196 – 209.

[39] Xu Z, Zhang Q, Fan C, et.al. A gel microparticle-based self-thickening strategy for 3D printing high-modulus hydrogels skeleton cushioned with PNAGA hydrogel mimicking anisotropic mechanics of meniscus. Bioactive Materials, 2023, 26: 64 – 76.

[40] Esmaeili J, Maedeh Rahimnejad, Riaz M, et.al. Development of 3D-printed biocompatible materials for meniscus substitution. Elsevier eBooks, Elsevier BV, 2024: 487 – 506.

[41] Guo W, Chen M, Wang Z, et. al. 3D-printed cell-free PCL–MECM scaffold with biomimetic micro-structure and micro-environment to enhance in situ meniscus regeneration. Bioactive Materials, 2021, 6 (10): 3620 – 3633.

[42] Chen M, Wu J, Yin H, et.al. [Construction of a novel tissue engineered meniscus scaffold based on low temperature deposition three-dimenisonal printing technology]. PubMed, National Institutes of Health, 2024, 38 (6): 748 – 754.

[43] Massonie M, Coline Pinese, Simon M, et.al. Biodegradable Tyramine Functional Gelatin/6 Arms-PLA Inks Compatible with 3D Two Photon-Polymerization Printing and Meniscus Tissue Regeneration. Biomacromolecules, American Chemical Society, 2024.

[44] Zhang Z-Z, Jiang D, Ding J, et.al. Role of scaffold means pore size in meniscus regeneration. 2016, 43: 314 – 326.

[45] Gopinathan J, Pillai M M, Shanthakumari S, et.al. Carbon nanofiber amalgamated 3D poly-ε-caprolactone scaffold functionalized porous-nanoarchitectures for human meniscal tissue engineering: In vitro and in vivo biocompatibility studies. Nanomedicine: Nanotechnology, Biology and Medicine, 2018, 14 (7): 2247 – 2258.

[46] Sooriyaarachchi D, Wu J, Feng A, et.al. Hybrid Fabrication of Biomimetic Meniscus Scaffold by 3D Printing and Parallel Electrospinning. Procedia Manufacturing, 2019, 34: 528 – 534.